JOC The Journal of Organic Chemistry

Article

pubs.acs.org/joc

Molecular Recognition of Aliphatic Diamines by 3,3′-Di(trifluoroacetyl)-1,1′-bi-2-naphthol

Shanshan Yu, Winston Plunkett, Michael Kim, Elaine Wu, Michal Sabat, and Lin Pu*

Department of Chemistry, University of Virginia, Charlottesville, Virginia 22904-4319, United States

Supporting Information

ABSTRACT: The fluorescent responses of 3,3′-di(trifluoroacetyl)-1,1′-bi-2-naphthol toward a variety of amines have been studied. It was found that the aliphatic primary 1,2- and 1,5-diamines can greatly enhance the fluorescence of this compound, but under the same conditions, primary, secondary, and tertiary monoamines cannot turn on the fluorescence of this compound. In addition, this compound was shown to be an enantioselective and diastereoselective fluorescent sensor for chiral diamines. UV absorption and NMR spectroscopic methods have been used to study the interaction of the sensor with amines. These studies have demonstrated that the intramolecular OH···O═C hydrogen bonding of the sensor is important for both the reactivity of its trifluoroacetyl group with the amines and its fluorescent responses. The interaction of both of the two amine groups of a diamine molecule with the sensor is essential for the observed fluorescent sensitivity and selectivity.

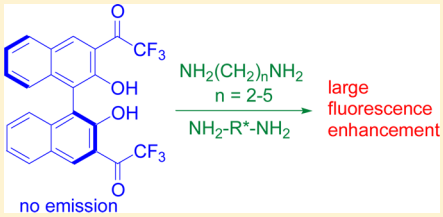

INTRODUCTION

Trifluoromethyl ketones contain a highly electrophilic trifluoroacetyl group whose reactions with a variety of nucleophiles have been utilized for the development of various types of molecular sensors. In 1974, the use of a trifluoromethyl aryl ketone for the selective electrochemical detection of carbonates was reported by Herman.[1] It was found that the nucleophilic addition of carbonates to the highly electrophilic trifluoromethyl ketone was responsible for the selective detection.[2] Trifluoromethyl aryl ketone-based membranes were used as optical sensors for humidity and ethanol as reported by Simon in 1991.[3] These sensors showed hypsochromic shifts of their absorption bands when water or ethanol was added to the trifluoroacetyl group to disrupt the conjugation system. Additional reports have appeared in recent years for the further development of trifluoromethyl ketone-based absorption and fluorescence sensors to recognize many nucleophilic species such as alcohols, amines, and various anions.[4] The use of a binaphthyl-based chiral trifluoromethyl ketone to distinguish the enantiomers of amino acids by NMR spectroscopic methods was also reported by Anh in 2010.[5] In spite of these studies, however, no study on the use of trifluoromethyl ketone-based molecules for enantioselective fluorescent recognition was reported before our recent work.[6] Enantioselective fluorescent sensors are potentially useful for rapid chiral assays, and significant progress has been made in this area over the past decade.[7,8] We recently communicated the use of 3,3′-di(trifluoroacetyl)-1,1′-binaphthol for the enantioselective fluorescent recognition of a chiral diamine.[6] We have demonstrated that using this trifluoroacetyl-based chiral sensor allowed a simultaneous determination of both the concentration and enantiomeric composition of the chiral diamine. In this paper, we report our detailed investigation of the interaction of the trifluoroacetyl compound with a variety of amines and diamines. This study has provided further understanding of the use of the trifluoromethyl ketone-based sensor for the molecular recognition of amines and diamines.

RESULTS AND DISCUSSION

1. Synthesis and Characterization of 3,3′-Di(trifluoroacetyl)-1,1′-bi-2-naphthol [(*S*)-4]. We prepared the 3,3′-trifluoromethyl ketone (*S*)-**4** from (*S*)-1,1′-bi-2-naphthol (BINOL) [(*S*)-**1**] according to Scheme 1. Protection of (*S*)-**1** with methoxymethyl (MOM) groups gave (*S*)-**2** in 95% yield.[9] Treatment of (*S*)-**2** with *n*-BuLi followed by addition of ethyl trifluoroacetate produced (*S*)-**3** as a yellow oil in 62% yield. The MOM groups of (*S*)-**3** were removed in the presence of CF_3COOH to generate the desired 3,3′-di(trifluoroacetyl)-BINOL (*S*)-**4** as an orange solid in 84% yield. Compound (*S*)-**4** gave a much greater specific optical rotation than (*S*)-**3**. The ^1H NMR spectrum of (*S*)-**4** in $CDCl_3$ revealed a deshield proton signal at δ 10.51 for the hydroxyl groups, consistent with a strong hydrogen-bonding interaction with the carbonyl groups. The hydroxyl proton signals of BINOL derivatives normally appear at δ <6. The ^{19}F NMR spectrum of (*S*)-**4** in $CDCl_3$ displayed a singlet at δ −70.06.

The UV absorption properties of a methylene chloride solution of (*S*)-**4** are compared with those of the MOM-protected compound (*S*)-**3** in Figure 1. For (*S*)-**3**, the absorptions were observed at λ_{max}/nm (ε/M^{-1} cm^{-1}) = 229 (5.8×10^4), 257 (4.4×10^4), 291 (1.7×10^4), and 357 (3.5×10^3). For (*S*)-**4**, the absorptions were observed at λ_{max}/nm (ε/M^{-1} cm^{-1}) = 228 (4.5×10^4), 263 (5.2×10^4), 319 (3.0×10^4), and 432 (4.8×10^3). As shown in the UV absorption spectrum of (*S*)-**3** in Figure 1, protection of the two hydroxyl groups of

Received: October 12, 2013
Published: November 27, 2013

Scheme 1. Synthesis of 3,3′-Di(trifluoroacetyl)-BINOL [(*S*)-4]

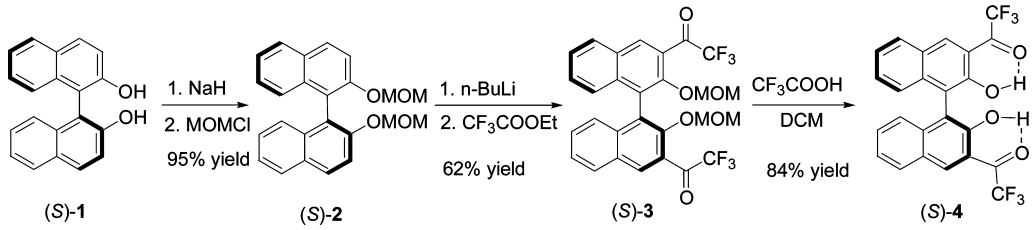

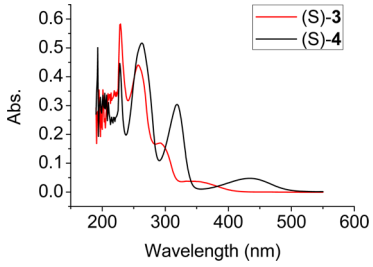

Figure 1. Comparison of the UV spectrum of (*S*)-**4** with that of (*S*)-**3** in CH_2Cl_2 (1.0×10^{-5} M).

(*S*)-**4** led to the disappearance of the longest-wavelength absorption at λ_{max} = 432 nm. Thus, this long-wavelength absorption can be attributed to the effect of the intramolecular OH···O═C hydrogen bonding in (*S*)-**4**. This hydrogen bonding should form a more planar conjugated system, and it could also make the hydroxyl group a better electron donor and the carbonyl group a better electron acceptor in comparison with those in (*S*)-**3**.

The fluorescence spectrum of (*S*)-**4** was also compared with that of (*S*)-**3** in CH_2Cl_2 at 1.0×10^{-5} M. As shown in Figure 2,

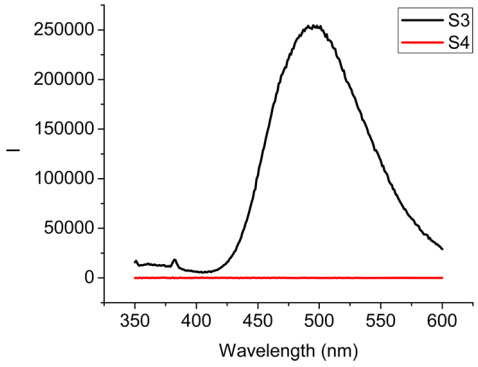

Figure 2. Fluorescence spectra of (*S*)-**3** and (*S*)-**4** in CH_2Cl_2 (1.0×10^{-5} M). (λ_{exc} = 343 nm, slit = 2.0/2.0 nm.)

although the MOM-protected compound (*S*)-**3** gave very strong emission at λ = 495 nm, (*S*)-**4** was not emissive at all. The emission of (*S*)-**3** is significantly red-shifted from that of BINOL observed at around 360 nm,[10] which could be attributed to its internal charge-transfer state arising from the incorporation of the trifluoroacetyl electron acceptor. Apparently, the intramolecular OH···O═C hydrogen bonding of (*S*)-**4** quenches its fluorescence.

We studied the solvent effect on the fluorescence properties of (*S*)-**4**. As shown in Figure 3, (*S*)-**4** gave very little emission in CH_2Cl_2, $CHCl_3$, and CH_3CN, moderate emission in THF and DMSO, and very strong emission in MeOH. Changing the solvent from CH_3CN to CH_3CN/H_2O (1:1) and from THF to

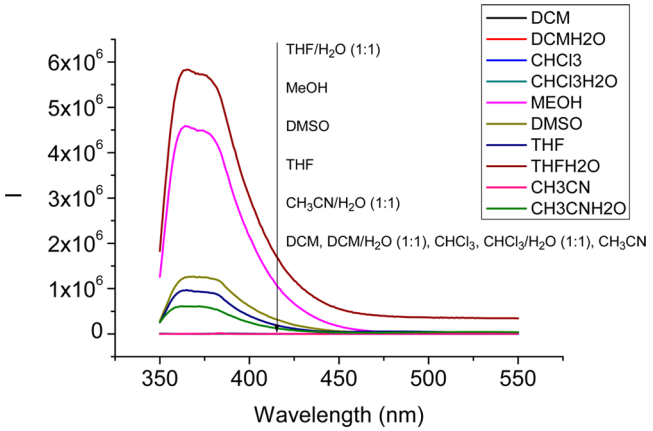

Figure 3. Fluorescence spectra of (*S*)-**4** in various solvents (1.0×10^{-5} M). (λ_{exc} = 343 nm, slit = 2.0/2.0 nm.)

THF/H_2O (1:1) caused large fluorescence enhancements. However, addition of H_2O to the CH_2Cl_2 or $CHCl_3$ solution of (*S*)-**4** did not affect its fluorescence, which could be attributed to the limited solubility of H_2O in these solvents. It is interesting to observe that when there was very weak or no emission, the solution was light yellow, but when there was strong emission, the solution became colorless.

The quenched fluorescence of compound (*S*)-**4** could be attributed to an excited-state intramolecular proton transfer process involving its intramolecular OH···O═C hydrogen bonding.[11] Absorption of photons frequently changes the electron distribution within a fluorophore.[12] Aromatic alcohols or protonated amines become more acidic in the excited state than in the ground state because the electrons on the hydroxyl group or protonated amine are shifted into the aromatic ring in the excited state.[13] Aromatic carboxylic acids and esters usually become more basic in the excited state because electron acceptors have vacant π^* orbitals into which electrons can be transferred. In the case of 2-naphthol, pK_a decreases from 9.2 in the ground state to 2.0 in the excited state.[14] In acid solution, the emission is from naphthol with an emission maximum at 357 nm. In basic solution, the emission is from the naphtholate anion with an emission maximum at 409 nm. At intermediate pH values, emission from both species is observed in water.[15] It has been shown that water clusters serves as proton acceptors, which explains why naphtholate emission disappears in nonaqueous solvents.[16] When a molecule contains both the proton donor and proton acceptor, excited-state proton transfer within the molecule is facile since the transferring proton is very close to the acceptor. For example, methyl 2-hydroxy-3-naphtholate (MNA), which contains both the proton donor and proton acceptor, is known to undergo an intramolecular excited-state proton transfer reaction.[17] The transferring proton, which is already hydrogen-bonded with ester group,

dx.doi.org/10.1021/jo402277p | J. Org. Chem. 2013, 78, 12671−12680

very easily moves to its adjacent oxygen atom in the excited state. This theory can also be applied to compound (*S*)-**4** because of its intramolecular hydrogen bonds. When methanol or water is added to (*S*)-**4**, nucleophilic attack on the highly electrophilic carbonyls could happen, which should change the structure of the original intramolecular hydrogen bond and thus change its fluorescent properties.

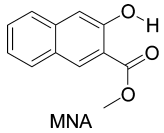

Scheme 2 shows a proposed mechanism for the fluorescence of (*S*)-**4**. In nonaqueous solution, the excited-state proton transfer of (*S*)-**4** upon irradiation could generate a nonemissive species **5**. In the presence of water, the hydrate compound **6** could be generated. The excited-state proton transfer of **6** upon irradiation could generate naphthalate **7**, which could be emissive.

Scheme 2. Proposed Mechanism for the Fluorescence of (*S*)-4

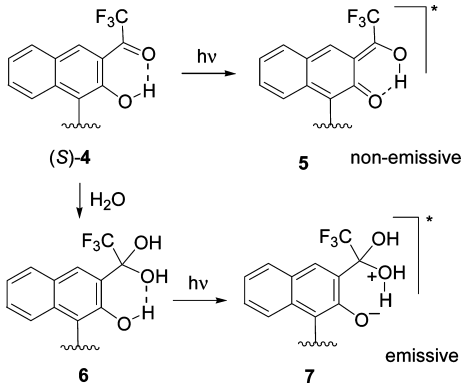

2. Interactions of (*S*)-4 with Amines. Earlier, we communicated our study of the fluorescent response of (*S*)-**4** toward the two enantiomers of *trans*-cyclohexane-1,2-diamine.[6] We further studied the interaction of (*S*)-**4** with the structurally diverse amines and diamines listed in Figure 4. These compounds include the tertiary, secondary, and primary monoamines **8**–**15**, the aliphatic diamines **16**–**20**, the aromatic diamine **21**, and the stereoisomeric aliphatic diamines **22** and **23**.

a. Fluorescence Study. When (*S*)-**4** (1.0×10^{-5} M in CH_2Cl_2) was treated with monoamines **8**–**15** (1.0×10^{-3} M), very little change in the fluorescence was observed (Figure 5a). However, when the aliphatic diamines **16**–**19** were used under the same conditions, large fluorescence enhancements were observed. Among these, ethylenediamine (**16**) and 1,5-diaminopentane (**19**) generated greater fluorescence enhancements than 1,3-diaminopropane (**17**) and 1,4-diaminobutane (**18**), and they produced dual emission signals for (*S*)-**4**, with λ = 370 nm and 438 nm (sh) for **16** and λ = 384 nm and 438 nm (sh) for **19**. Both diamines enhanced the short-wavelength emission more than the long-wavelength emission. The fluorescence enhancements by the other two diamines, **17** and **18**, were only 3% of that by **16**. The benzylic diamine **20** and the aromatic diamine **21** did not turn on the fluorescence at all.

We compared the fluorescence responses of (*S*)-**4** toward the previously reported *trans*-cyclohexane-1,2-diamine isomers (*R*,*R*)-**22** and (*S*,*S*)-**22** with those toward *meso-cis*-cyclohexane-1,2-diamine [(*S*,*R*)-**22**]. As shown in Figure 5b, these three stereoisomers gave very interesting fluorescence enhancements. All three isomers turned on the fluorescence of (*S*)-**4** and showed dual emission at λ_1 = 370 and λ_2 = 438 nm, but the fluorescent responses at the two emission wavelengths were different. (*R*,*R*)-**22** caused large fluorescence enhancements at both λ_1 and λ_2, with the intensity at λ_1 being smaller than that at λ_2. (*S*,*S*)-**22** enhanced λ_1 greatly but resulted in a much smaller enhancement at λ_2. The *meso* isomer (*S*,*R*)-**22** enhanced λ_1 greatly, and the enhancement at λ_2 was a little smaller. Similarly, both enantiomers of chiral 1,2-diaminopropane **23** caused significant fluorescence enhancement at both λ_1 and λ_2, with (*R*)-**23** providing greater enhancement than (*S*)-**23** at λ_2 (Figure 5c).

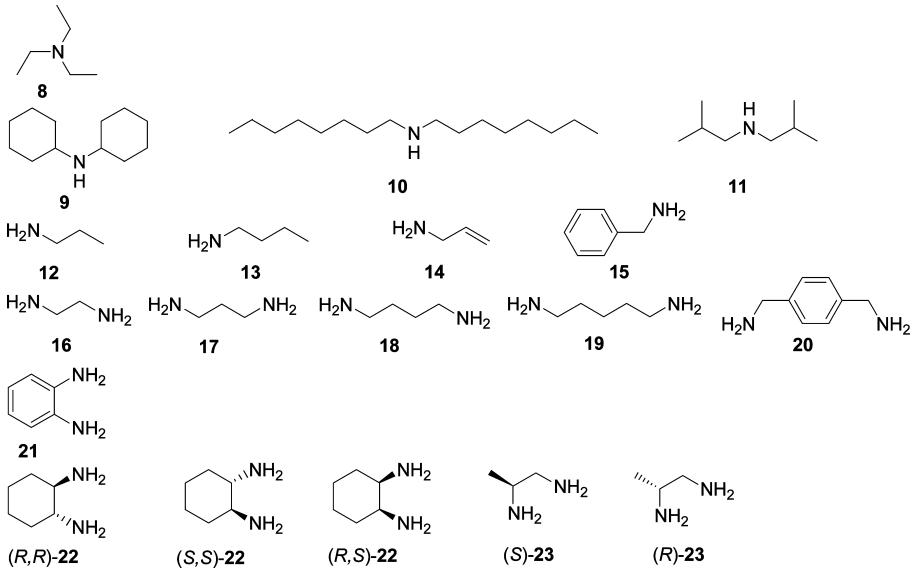

Figure 4. Structures of the various amines investigated.

dx.doi.org/10.1021/jo402277p | *J. Org. Chem.* 2013, 78, 12671–12680

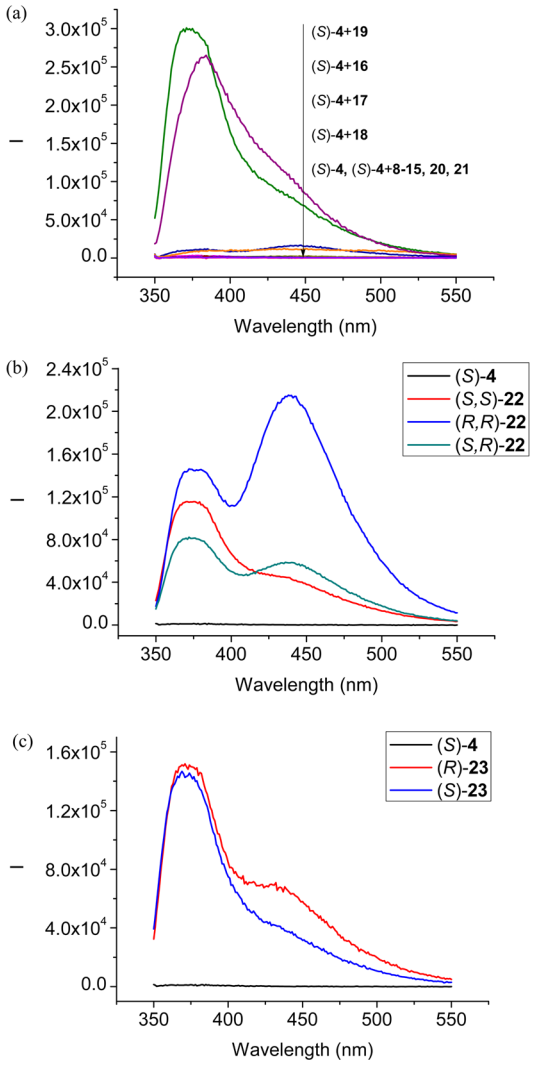

Figure 5. Fluorescence spectra of (*S*)-**4** (1.0×10^{-5} M) in the presence of (a) various achiral amines **8**–**21**, (b) three stereoisomers of **22**, and (c) two enantiomers of **23** (1.0×10^{-3} M). (λ_{exc} = 343 nm, slit = 2.0/2.0 nm.)

We studied the effect of the concentration of the three stereoisomers of cyclohexane-1,2-diamine on I_1/I_2, the ratio of the fluorescence intensities at the two emission wavelengths. As shown in Figure 6, the I_1/I_2 ratio remained constant while the concentrations of these three stereoisomers varied, with I_1/I_2 = 0.67 for (*R*,*R*)-**22**, 2.60 for (*S*,*S*)-**22**, and 1.38 for (*S*,*R*)-**22**. Therefore, using the value of the I_1/I_2 ratio, we can distinguish the three stereoisomers of cyclohexane-1,2-diamine without the need to determine their concentrations.

A similar study was also conducted on the fluorescence response of (*S*)-**4** toward the chiral diamine **23** in the concentration range of 5.0×10^{-4} to 5.0×10^{-3} M. Plots of the fluorescence intensity of (*S*)-**4** at λ_1 versus the concentrations of (*R*)- and (*S*)-**23** (Figure 7a) show that I_1 is strongly dependent on the concentration of the diamine but not on its chiral configuration. Plots of the fluorescence intensity at λ_2 versus the concentrations of (*R*)- and (*S*)-**23** (Figure 7b) show significant enantioselectivity for this emission signal. We also found that the I_1/I_2 ratio remained at 3.3–3.7 for (*S*)-**23** and 2.3–2.1 for (*R*)-**23** over the concentration range of 5.0×10^{-4} to 5.0×10^{-3} M.

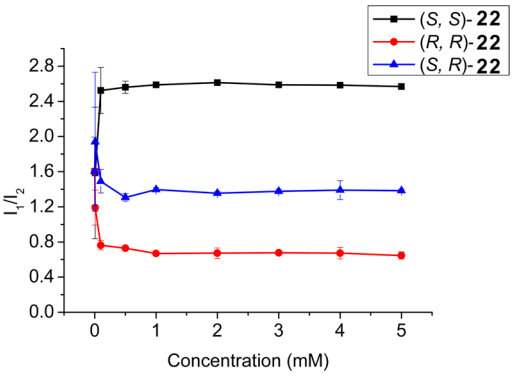

Figure 6. Plots of the I_1/I_2 ratio for (*S*)-**4** (1.0×10^{-5} M) in the presence of varying concentrations of (*R*,*R*)-, (*S*,*R*)-, and (*S*,*S*)-**22**. (I_1 and I_2 are the fluorescence intensities at λ_1 = 370 nm and λ_2 = 438 nm, respectively. Solvent: CH_2Cl_2. λ_{exc} = 343 nm, slit = 2/2 nm.)

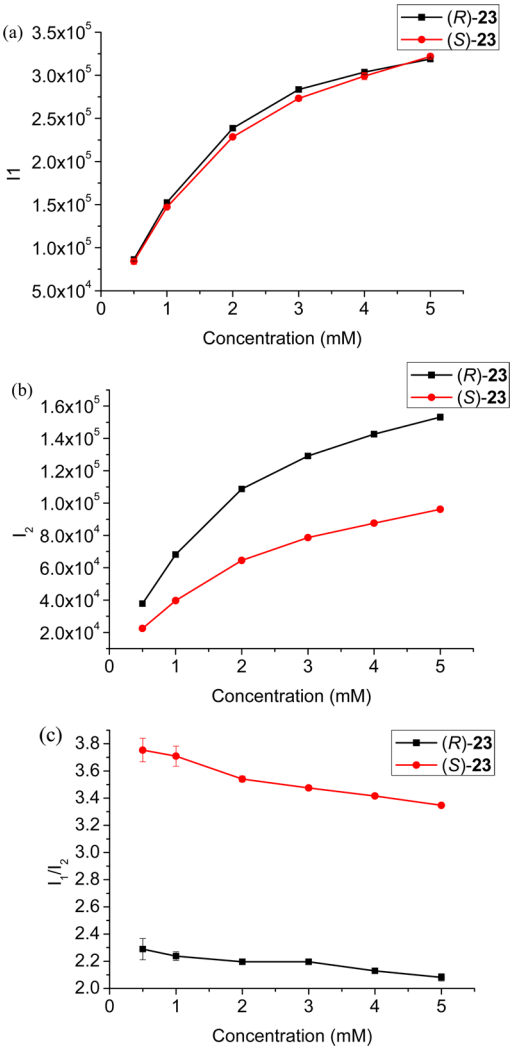

Figure 7. Plots of (a) I_1, (b) I_2 and (c) I_1/I_2 for (*S*)-**4** (1.0×10^{-5} M) in the presence of varying concentrations of (*R*)- and (*S*)-**23**. (I_1 and I_2 are the fluorescence intensities at λ_1 = 370 nm and λ_2 = 438 nm, respectively. Solvent: CH_2Cl_2. λ_{exc} = 343 nm, slit = 2/2 nm.)

In order to better understand the origin of the dual emission responses of (*S*)-**4** when treated with the diamines, excitation spectra were recorded for (*S*)-**4** in the presence of (*R*,*R*)- and (*S*,*S*)-**22**. As shown in Figure 8, for each sample, the same

dx.doi.org/10.1021/jo402277p | J. Org. Chem. 2013, 78, 12671–12680

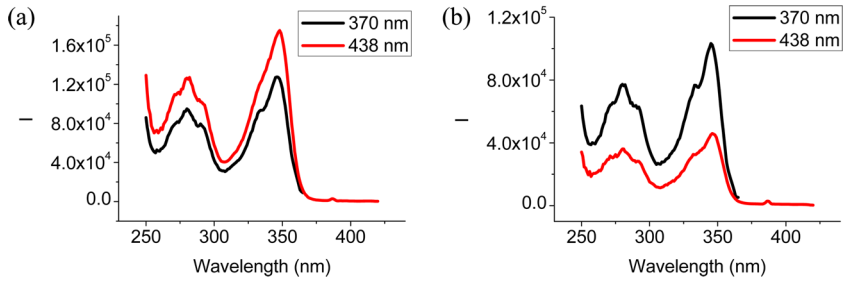

Figure 8. Excitation spectra of (*S*)-**4** in CH_2Cl_2 (1.0×10^{-5} M) in the presence of (a) (*R*,*R*)- or (b) (*S*,*S*)-**22** (4.0×10^{-3} M). (Slit = 2.0/2.0 nm.)

excitation spectrum was obtained for emission at either 370 or 438 nm. This indicates that the emissions at the two wavelengths should result from excitation of the same ground-state species. The fluorescence lifetimes of (*S*)-**4** in the presence of chiral diamine **22** were measured and found to be 1 ns for the emission at 370 nm and 1.7 ns for the emission at 438 nm. The difference in the lifetimes suggests that the two emission peaks should be from two different emitting states.

b. UV Study. We studied the effect of the amines on the UV absorptions of (*S*)-**4** in CH_2Cl_2. For monoamines **8**−**15** and diamines **20** and **21**, the UV spectra of the mixtures are simple additions of that of (*S*)-**4** with those of the amines. Thus, these compounds did not cause significant changes in the absorption of (*S*)-**4**. Aliphatic diamines **16**−**19** and the three stereoisomers of chiral diamine **22** caused big changes in the UV absorptions of (*S*)-**4** with similar patterns (Figures S2 and S3 in the Supporting Information). They included a significant decrease in the absorbance intensity at λ_{max} = 263, 319, and 432 nm, an increase at 231 nm, and the appearance of a new absorption peak at 345 nm. This demonstrates that these aliphatic diamines generated significant structural changes of (*S*)-**4** in the ground state. The decreased absorption at the longest-wavelength absorption of (*S*)-**4** indicates the disruption of the conjugation of the chromophore upon the addition of the diamine.

c. NMR Study. We conducted ^{19}F NMR titrations of (*S*)-**4** with **16**, **19**, and the three stereoisomers of **22** in $CDCl_3$. The $CDCl_3$ solution of (*S*)-**4** (0.4 mL, 5.0 mM) was prepared in an NMR tube. The $CDCl_3$ solution of the diamine (1 mL, 0.5 M) was prepared in a small vial as a stock solution. The NMR spectrum of (*S*)-**4** was first recorded, and then the stock solution of the diamine was gradually added to the NMR tube. After each addition, the solution was mixed well and the NMR spectrum was recorded.

(*S*)-**4** showed a singlet ^{19}F signal at δ −70.06. With the addition of 0.2 equiv of **16**, two peaks at δ −69.98 and −83.64 appeared with the same integration. These two new peaks kept increasing while the signal at δ −70.06 decreased until 0.8 equiv of **16** had been added. These two peaks were assigned to the monohemiaminal product **24** on the basis of a comparison with the literature data (Scheme 3).[16] Next, a new peak at δ −83.53 started to show up and all of the other signals decreased until 7.1 equiv of **16** had been added, at which point all of the other signals were converted to the peak at δ −83.53. This signal was assigned to the dihemiaminal product **25**.[18] Further addition of amine generated new peaks at around δ −72.58 and −80.20, which were assigned to the imine **26**[19] and the aminal **27**,[20] respectively. The signal at δ −72.58 remained at low intensity all the time, and the signal at around δ −80.20 increased while the signal at δ −83.53 decreased. This indicates that once the hemiaminal was converted to the imine, the imine was quickly

Scheme 3. Proposed Reaction of (*S*)-4 with Ethylenediamine

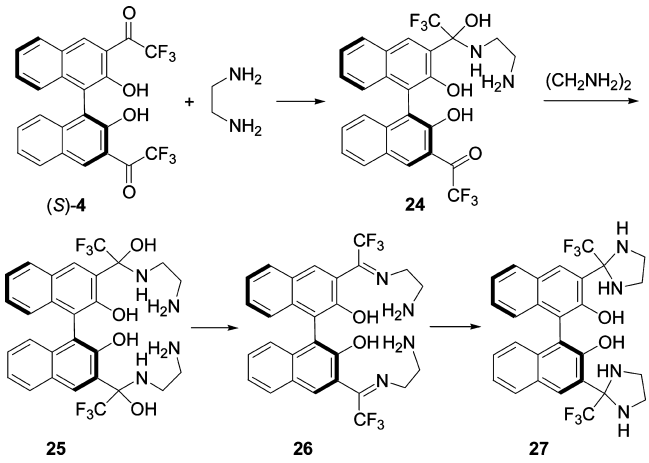

converted to the aminal . After 108 equiv of the amine had been added over 2 h, there was still an intense peak at δ −83.44 (shifted slightly from δ −83.53 in the presence of the excess amine). After the solution was allowed to stand overnight, the hemiaminal signal was significantly reduced while the aminal signal was increased, indicating that the conversion from the hemiaminal **25** to the aminal **27** proceeded slowly.

The formation of the 1:2 adduct between (*S*)-**4** and ethylenediamine (**16**) as shown in Scheme 3 is consistent with the Job plot obtained for the fluorescence response of (*S*)-**4** with the diamine at a total concentration of 0.1 mM (Figure 9). This plot demonstrates that the fluorescence emission reached a maximum at ∼30% (*S*)-**4** for its interaction with the diamine, indicating a (*S*)-**4**:**16** binding stoichiometry of 1:2.

The NMR titration of (*S*)-**4** with the three stereoisomers of **22** exhibited responses similar to those with ethylenediamine.[6] As shown in Scheme 4, we observed that the reaction of (*S*)-**4** with (*S*,*S*)-**22** gave hemiaminal **28** quickly. Compound **28** was

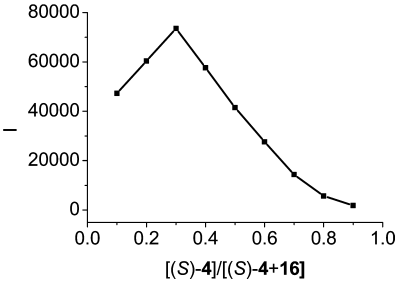

Figure 9. Job plot for the fluorescent response of (*S*)-**4** with ethylenediamine (**16**) (total concentration = 0.1 mM, λ_{exc} = 343 nm, slit = 2.0/2.0 nm).

dx.doi.org/10.1021/jo402277p | J. Org. Chem. 2013, 78, 12671−12680

Scheme 4. Proposed Mechanism for the Reaction of (*S*)-4 with (*S,S*)-22

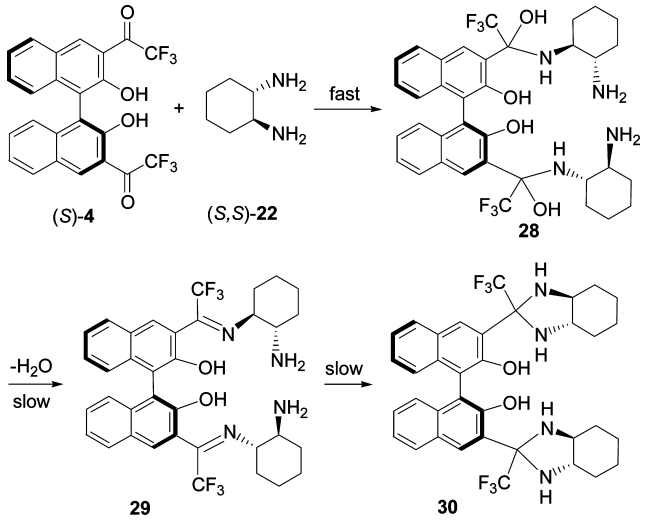

then converted to imine **29** slowly over 12 h and then to aminal **30** over several days. Compound **30** can be prepared by carrying out the reaction of (*S*)-**4** with (*S,S*)-**22** in the presence of molecular sieves at room temperature. The fluorescence spectrum of the aminal product **30** was obtained, and it contained a single emission peak at λ = 383 nm in CH_2Cl_2 with stronger intensity than those of the intermediates.

The NMR titration of (*S*)-**4** with 1,5-diaminopentane (**19**) showed more complicated signal changes. With addition of 0.19 equiv of **19**, a new peak at δ −83.81 appeared, and the signal of (*S*)-**4** became a little broader; it continued to become broader and shifted upfield with more amine addition. After the addition of 0.94 equiv of **19**, two new peaks at δ −85.80 and −86.65 appeared. When the amount of added amine increased to 5.3 equiv, the broad peak completely disappeared and only three peaks at δ −83.80, −85.81, and −86.41 were left. When even more amine was added, the NMR spectrum became more complex. The Job plot for the fluorescent response of (*S*)-**4** toward **19** at a total concentration of 0.1 mM was obtained. As shown in Figure 10, the maximum fluorescence was observed at

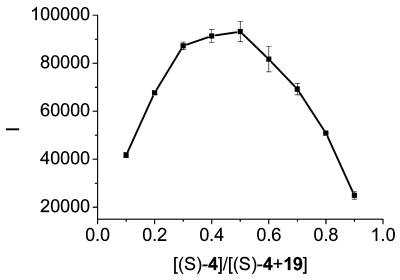

Figure 10. Job plot for the fluorescent response of (*S*)-**4** with **19** (total concentration = 0.1 mM, λ_{exc} = 343 nm, slit = 2.0/2.0 nm).

50% (*S*)-**4** for the interaction with **19**, and the fluorescence emission stayed high in the range of 30−50% (*S*)-**4**. This indicates a complicated binding mode between (*S*)-**4** and **19**, and both 1:1 and 1:2 (*S*)-**4**:**19** binding stoichiometries could exist in this system.

Thus, (*S*)-**4** should have multiple modes of reaction with **19**. Scheme 5 shows some possible reaction pathways that could lead to 1:1 and 1:2 adducts. Compound **31** represents one

Scheme 5. Proposed Reactions between (*S*)-4 and 1,5-Diaminopentane

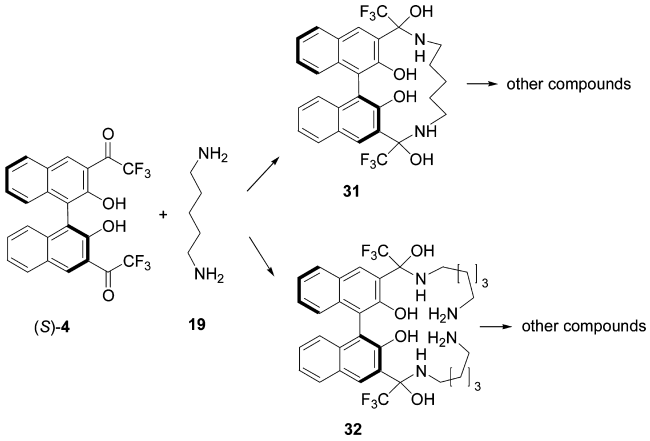

possible structure for the 1:1 adduct that could be generated from the addition of one molecule of the diamine to both of the $COCF_3$ groups of (*S*)-**4**. Other products such as **32**, imines, and oligomers could also be generated to give the complex ^{19}F NMR spectrum.

d. X-ray Structures. Crystals of the aminal product **30** isolated from the reaction of (*S*)-**4** with (*S,S*)-**22** were obtained by slow evaporation of its chloroform solution and used for X-ray analysis. Crystals of the final addition products for the reactions of (*S*)-**4** with ethylenediamine (**16**) and propylenediamine (**17**) were obtained by mixing the sensor with the diamines in a 1:10 ratio in chloroform followed by slow evaporation. The X-ray analyses of these crystals confirmed their bis(cyclic aminal) structures, as shown in Figure 11 for **30**. In these structures, the dihedral angles of the binaphthyl units are all 110°.

e. Discussion of the Interactions of (S)-4 with the Diamines. Our study of the interactions of (*S*)-**4** with various amines demonstrated that the reactions of (*S*)-**4** with aliphatic primary diamines are much more facile than those with other amines and give large fluorescence enhancements. The

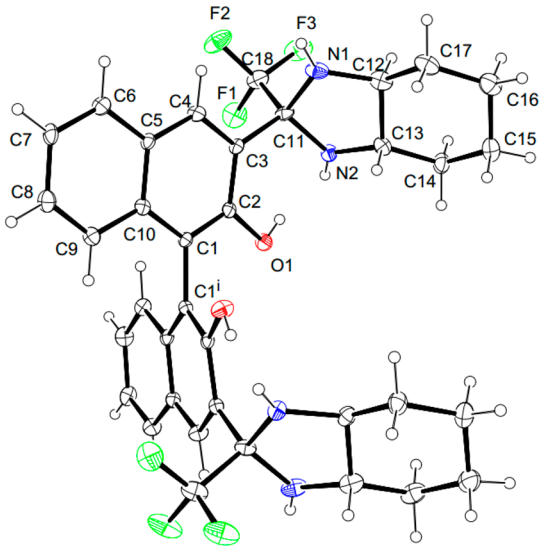

Figure 11. X-ray structure of the aminal product of (*S*)-**4** with (*S,S*)-**22**.

dx.doi.org/10.1021/jo402277p | *J. Org. Chem.* 2013, 78, 12671−12680

Scheme 6. Proposed Mechanism for the Reaction of (*S*)-4 with a 1,2-Diamine

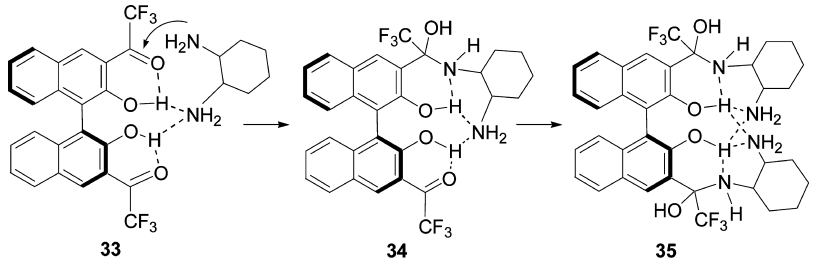

fluorescence responses of (*S*)-**4** toward the 1,2- and 1,5-diamines are much greater than those toward the 1,3- and 1,4-diamines. It is proposed that the intermolecular hydrogen bond between one of the amine groups of a 1,2-diamine molecule with the hydroxyl groups of the sensor, as shown by **33** in Scheme 6, should facilitate the addition of the second amine group to the trifluoroacetyl group. In the resulting adducts **34** and **35**, the original O−H···O═C hydrogen bonds in (*S*)-**4** have been disrupted to generate the observed fluorescence enhancement. That is, although the O−H···O═C hydrogen bonds of the sensor completely quench its fluorescence, the new O−H···N hydrogen bonds do not. The multiple hydrogen bonds shown by **35** could also contribute to the fluorescence enhancement through the increased structural rigidity. The interaction of both of the amine groups of the diamine with the sensor as shown in **35** could also explain the observed highly stereoselective fluorescent responses in the recognition of cyclohexane-1,2-diamine. That is, the chirality around the amine groups should lead to significant differences in the stability of the diastereomeric adducts **35**, giving the observed stereoselective fluorescent responses. When the 1,3- and 1,4-diamines are used, there may be greater ring strain for the hydrogen-bonding interactions of the second amine with the BINOL hydroxyl groups in the corresponding interactions similar to **33**−**35**, leading to the reduced fluorescence enhancements. When the 1,5-diamine was used, the observed large fluorescence enhancement could be attributed to the formation of a compound like **31** where both carbonyl groups of the sensor react with the amine to generate a more rigid macrocyclic structure.

*f. Interaction of the MOM-Protected Compound (S)-**3** with **22***. We also studied the interaction of the MOM-protected compound (*S*)-**3** with the chiral diamines (*R*,*R*)- and (*S*,*S*)-**22** in CH_2Cl_2. Without the intramolecular OH···O═C hydrogen bonds of (*S*)-**4**, (*S*)-**3** was strongly emissive. Both enantiomers of **22** only slightly quenched the fluorescence of (*S*)-**3** (by ~10%) with no enantioselectivity (Figure 12). The UV spectrum of (*S*)-**3** showed little change in the presence of (*R*,*R*)- or (*S*,*S*)-**22**. This demonstrates that without the hydroxyl groups, there was little reaction between the amine group and the trifluoroacetyl group. Thus, the hydroxyl groups of (*S*)-**4** could play multiple roles in the fluorescent recognition of the diamines, as listed below: (1) They form intramolecular hydrogen bonds with the carbonyl groups to quench the fluorescence of (*S*)-**4**, which can then be turned on upon interaction with the diamine. (2) These *intra*molecular hydrogen bonds could activate the carbonyl groups for the nucleophilic addition of the diamine. (3) The hydroxyl groups can form *inter*molecular hydrogen bonds with one of the amine groups of the diamine to accelerate the reaction. (4) After the addition of one of the amine groups of the diamine to the

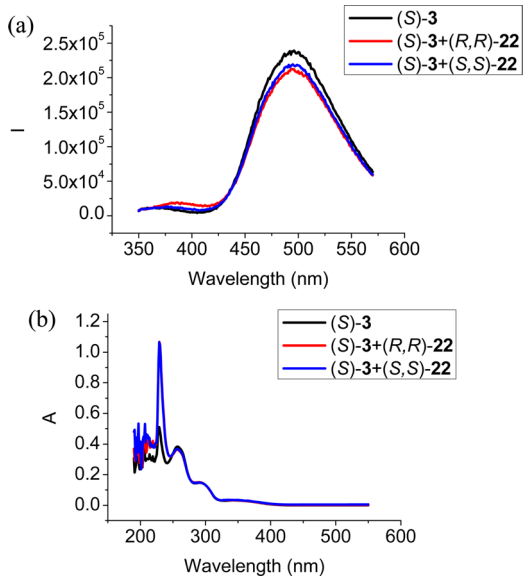

Figure 12. (a) Fluorescence spectra of (*S*)-**3** in the presence of (*R*,*R*)- or (*S*,*S*)-**22** (λ_{exc} = 343 nm, slit = 2.0/2.0 nm). (b) UV spectra of (*S*)-**3** in the presence of (*R*,*R*)- or (*S*,*S*)-**22**. [(*S*)-**3**: 1.0×10^{-5} M in CH_2Cl_2. Amine: 5.0×10^{-3} M.)

trifluoroacetyl group of (*S*)-**4**, the hydrogen bonds of the second amine group with the hydroxyl groups of (*S*)-**4** could increase the structural rigidity of the diamine addition products to further enhance the fluorescence.

When the excitation wavelength was changed to 290 nm, the MOM-protected compound (*S*)-**3** showed dual emissions at λ = 359 and 494 nm, in which the emission at 359 nm was much weaker than that at 494 nm (Figure 13). We attribute the short-wavelength emission to the locally excited state of the naphthol units and the long-wavelength emission to the internal charge-transfer state of the conjugated donor (OMOM) and acceptor

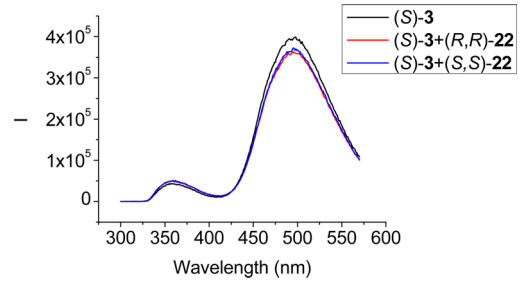

Figure 13. Fluorescence spectra of (*S*)-**3** in CH_2Cl_2 (1.0×10^{-5} M) in the presence of (*R*,*R*)- or (*S*,*S*)-**22** (5.0×10^{-3} M) at λ_{exc} = 290 nm (slit = 2.0/2.0 nm).

dx.doi.org/10.1021/jo402277p | *J. Org. Chem.* 2013, 78, 12671−12680

($COCF_3$) units. Only very small changes were observed at both wavelengths in the presence of **22**.

g. Further Study of the Interaction of (S)-4 with Propylamine at High Concentrations. As discussed above, the aliphatic primary diamines such as **16**, **19**, and **22** reacted with (*S*)-**4** readily to greatly enhance its fluorescence. However, the monoamines at 1.0×10^{-3} M could not turn on the fluorescence of (*S*)-**4**, as shown in Figure 5a. At this concentration, they also did not cause any change in the UV spectrum of (*S*)-**4**. In order to gain additional understanding of the reaction of (*S*)-**4** with the amines, we explored the use of much higher concentrations of a monoamine, propylamine (**12**), to interact with (*S*)-**4**. Figure 14a shows that when the concentration of propylamine was increased over 5.0×10^{-3} M, the fluorescence of (*S*)-**4** (1.0×10^{-5} M in CH_2Cl_2) at λ = 380 nm could be turned on, although the overall intensity was still much weaker than that in the presence of the aliphatic diamines. As the concentration of propylamine increased, a significant fluorescence enhancement of the long-wavelength emission (λ = 436 nm) of the sensor was also observed. At high concentrations of propylamine, the UV absorptions of (*S*)-**4** underwent significant changes. As shown in Figure 14b, in the presence of 5.0×10^{-2} M propylamine, the long-wavelength absorption of (*S*)-**4** at λ = 432 nm diminished, accompanied by the appearance of a new peak at 348 nm and decreases at 263 and 319 nm. These changes were very similar to those observed for the interaction of **16** and **22** with (*S*)-**4**. These results suggest that monoamines and diamines should cause similar structural changes to (*S*)-**4** but that much higher concentrations are needed for the use of the monoamines.

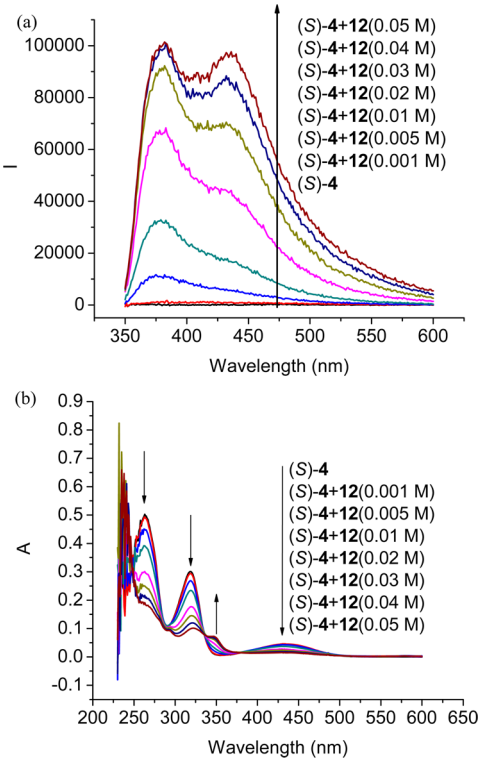

Figure 14. (a) Fluorescence spectra of (*S*)-**4** (1.0×10^{-5} M in CH_2Cl_2) in the presence of propylamine at 0–0.05 M (λ_{exc} = 343 nm, slit = 2.0/2.0 nm). (b) UV–vis absorption spectra of (*S*)-**4** (1.0×10^{-5} M in CH_2Cl_2) in the presence of propylamine at 0–0.05 M.

We conducted an ^{19}F NMR study of the reaction of (*S*)-**4** with propylamine. For the NMR study, a much higher concentration of (*S*)-**4** (5 mM) in $CDCl_3$ than used in the fluorescence and UV experiments (10^{-5} M) was needed for the signal detection. However, at this high concentration, when (*S*)-**4** was treated with propylamine, the NMR spectrum showed the disappearance of the signal of (*S*)-**4** with formation of a very weak and broad signal. Sometimes the formation of a yellowish precipitate could be observed. This indicates that the solubility of the addition product of (*S*)-**4** with propylamine should be lower than the detection limit of the NMR experiments for characterization. In order to characterize the product of the reaction of (*S*)-**4** with propylamine, we switched the solvent to DMSO-d_6 for the ^{19}F NMR titration of (*S*)-**4** with propylamine. In DMSO-d_6, the ^{19}F NMR spectrum of (*S*)-**4** showed multiple signals, probably due to the reaction of the nucleophilic solvent and water molecules with the trifluoroacetyl groups of (*S*)-**4**. Addition of 20 equiv of propylamine converted all of the signals to a singlet at δ −81.51. ^1H and ^{13}C NMR spectra for the reaction of (*S*)-**4** with propylamine in DMSO-d_6 suggested a dihemiaminal structure for the reaction product **36** (see page S32 in the Supporting Information). The mass spectrum of the compound indicated that compound **36** might not be stable upon isolation, with a base peak at *m*/*z* 538.1 attributed to the loss of one of the two propylamine groups of **36** (see page S33 in the Supporting Information).

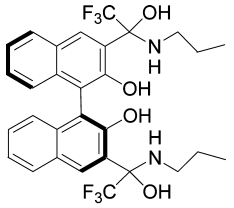

36

On the basis of these studies, the mechanism shown in Scheme 7 is proposed to explain the fluorescence responses of (*S*)-**4** toward propylamine shown in Figure 14a. The observed initial fluorescence enhancement of the short-wavelength emission (λ = 380 nm) could be attributed to the formation of the hemiaminal adduct **36**. Further interaction of this adduct

Scheme 7. Proposed Interaction of (*S*)-4 with Propylamine

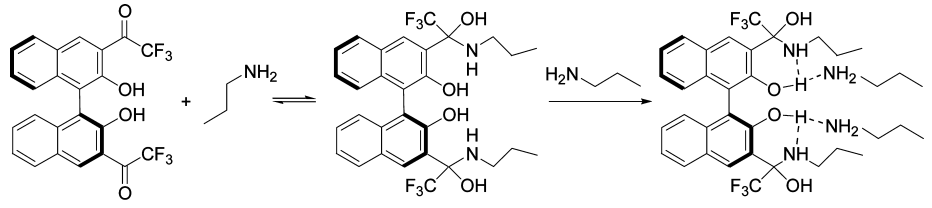

(*S*)-**4** **36** **37**

dx.doi.org/10.1021/jo402277p | J. Org. Chem. 2013, 78, 12671–12680

with additional amine molecules to form a hydrogen-bonded complex such as **37** could contribute to the observed fluorescence enhancement of the long-wavelength emission (λ = 436 nm).

The study of the fluorescent response of (*S*)-**4** toward propylamine at high concentrations could be used to explain the observed dual emissions of (*S*)-**4** in the presence of the aliphatic diamines. That is, the nucleophilic addition of one amine group of a diamine molecule to the trifluoroacetyl group of (*S*)-**4** should be responsible for the fluorescence enhancement at the short wavelength, while the hydrogen-bonding interaction of the second amine group of the diamine with the hydroxyl groups of the sensor should be responsible for the fluorescence enhancement of the long-wavelength emission.

SUMMARY

We have demonstrated that the trifluoromethyl BINOL ketone (*S*)-**4** is not only an enantioselective fluorescent sensor for chiral 1,2-diamines but can also be used to distinguish aliphatic 1,2- to 1,5-diamines from aromatic diamines and primary, secondary, and tertiary monoamines. This study has shown that the intramolecular OH···O═C hydrogen bonding of the sensor is important for both the reactivity of the trifluoroacetyl group with the amines and the fluorescent response of the sensor. The interaction of both of the amine groups of a diamine molecule with the sensor is essential for the observed fluorescent sensitivity and selectivity. This work has shed new light on the trifluoromethyl ketone-based molecular sensors.

EXPERIMENTAL SECTION

General Data. Reactions were carried out under nitrogen unless otherwise noted. THF was distilled over sodium and benzophenone under a nitrogen atmosphere. Methylene chloride and diethyl ether were dried by passage through activated alumina columns under nitrogen. Solvents were stored over 4 Å molecular sieves. Chemical shifts for ^{1}H NMR spectra are reported in parts per million relative to a singlet at 7.26 ppm for deuterated chloroform. Chemical shifts for ^{13}C NMR were reported relative to the center line of a triplet at 77.16 ppm for deuterated chloroform. The ^{19}F NMR spectra are reported in parts per million relative to trifluoroacetic acid (δ −76.55) as an external reference.

Preparation of Samples for Fluorescence Measurements. Sensors were purified by column chromatography followed by recrystallization and then stored in a refrigerator. All of the solvents were either HPLC or spectroscopic grade. Stock solutions of the sensors were freshly prepared for each measurement. For the fluorescence study, a sensor solution was mixed with the amine solution at room temperature in a 5 mL volumetric flask and diluted to the desired concentration. The resulting solution was allowed to stand at room temperature for 0.5 h before the fluorescence measurement, and all of the fluorescence spectra were taken within 2 h.

Synthesis and Characterization of Compounds. *Synthesis and Characterization of (S)-**2**.* Under nitrogen, (*S*)-BINOL [(*S*)-**1**] (17.5 mmol, 5.0 g) was dissolved in THF (200 mL). The solution was cooled to 0 °C, and NaH (43.75 mmol, 60% in mineral oil, 1.75 g) was added in small portions. The reaction mixture was stirred for 15 min, and then chloromethyl methyl ether (43.75 mmol, 3.3 mL) was added slowly. The reaction mixture was allowed to warm to room temperature and stirred for 1 h. Water was added slowly to quench the reaction. The organic layer was separated, and the aqueous layer was extracted with ethyl acetate (3 × 30 mL). The combined organic extracts were washed with brine and dried over Na_2SO_4. After evaporation of the solvent, the residue was purified by column chromatography on silica gel eluted with hexane/ethyl acetate (15/1) to afford compound (*S*)-**2** as a white solid in 95% yield (16.6 mmol, 6.22 g). The NMR data of the compound matched those reported.[9a]

*Synthesis and Characterization of (S)-**3**.* Under nitrogen, 2,2′-bis(methoxymethyl)-1,1′-binaphthyl [(*S*)-**2**] (3.0 mmol, 1.12 g) was dissolved in diethyl ether (36 mL). The solution was cooled to 0 °C, and *n*-BuLi (12.0 mmol, 2.5 M in hexane, 4.8 mL) was added dropwise. The reaction mixture was stirred for 2 h at room temperature and cooled to 0 °C, and then ethyl trifluoroacetate (13.5 mmol, 1.6 mL) was added slowly. The reaction mixture was allowed to warm to room temperature and stirred for 1 h to afford a creamlike mixture. A saturated aqueous NH_4Cl solution was added to quench the reaction. The organic layer was separated, and the aqueous layer was extracted with ethyl acetate (3 × 20 mL). The combined organic extracts were washed with brine and dried over Na_2SO_4. After evaporation of the solvent, the residue was purified by column chromatography on silica gel eluted with hexane/methylene chloride (1/3) to afford compound (*S*)-**3** as a yellow oil in 62% yield (1.86 mmol, 1.05 g). ^{1}H NMR (300 MHz, $CDCl_3$): δ 2.77 (s, 6H), 4.73 (d, J = 6.3 Hz, 2H), 4.77 (d, J = 6.3 Hz, 2H), 7.25 (d, J = 8.7 Hz, 2H), 7.44−7.50 (m, 2H), 7.53−7.58 (m, 2H), 8.05 (d, J = 8.1 Hz, 2H), 8.43 (s, 2H). ^{19}F NMR (282 MHz, $CDCl_3$): δ −73.62. ^{13}C NMR (75 MHz, $CDCl_3$): δ 56.6, 100.7, 116.5 (q, J = 290 Hz), 126.4, 126.8, 126.9, 127.0, 129.6, 129.8, 130.1, 132.7, 136.2, 151.6, 182.4 (q, J = 35.6 Hz). HRMS Calcd for $C_{28}H_{20}O_6F_6Na$ (MNa^+): 589.1062. Found: 589.1053. $[\alpha]_D$ = −18.06 (c = 0.590, $CHCl_3$).

*Synthesis and Characterization of (S)-**4**.* After compound (*S*)-**3** (0.25 mmol, 134.2 mg) was dissolved in a minimum amount of CH_2Cl_2, trifluoroacetic acid (1.0 mL) was added slowly, and the mixture was stirred at room temperature for 10 min. A saturated aqueous $NaHCO_3$ solution was added to quench the reaction. The organic layer was separated, and the aqueous layer was extracted with CH_2Cl_2 (3 × 20 mL). The combined organic extracts were washed with brine and dried over Na_2SO_4. After evaporation of the solvent, the residue was purified by column chromatography on silica gel eluted with hexane/methylene chloride (2/1) to afford compound (*S*)-**4** as an orange solid in 84% yield (0.21 mmol, 100 mg). ^{1}H NMR (300 MHz, $CDCl_3$): δ 7.16 (d, J = 7.5 Hz, 2H), 7.41−7.51 (m, 4H), 8.02 (d, J = 7.5 Hz, 2H), 8.70 (s, 2H), 10.51 (s, 2H). ^{19}F NMR (282 MHz, $CDCl_3$): δ −70.06. ^{13}C NMR (150 MHz, $CDCl_3$): δ 115.2, 116.7 (q, J = 289.5 Hz), 117.8, 124.7, 125.3, 127.2, 131.2, 132.2, 136.1 (q, J = 3.75 Hz), 138.5, 155.0, 185.1 (q, J = 36.0 Hz). HRMS Calcd for $C_{24}H_{13}O_4F_6$ (MH^+): 479.0718. Found: 479.0719. Mp: 231 °C. $[\alpha]_D$ = −167.50 (c = 0.355, $CHCl_3$).

*Synthesis and Characterization of **30**.* Under nitrogen, (*S*)-**4** (0.1 mmol, 47.8 mg) was dissolved in CH_2Cl_2 (3 mL). (*S*,*S*)-**22** (2.0 mmol, 228.4 mg) and 4 Å molecular sieves were added. The reaction mixture was stirred for 2 days at room temperature. After filtration, the solvent was evaporated, and the residue was purified by column chromatography on neutral aluminum oxide eluted with methylene chloride to afford compound **30** as a white solid in 65% yield. ^{1}H NMR (300 MHz, $CDCl_3$): δ 1.20−1.34 (m, 8H), 1.84−1.87 (m, 4H), 2.06−2.09 (m, 2H), 2.25−2.29 (m, 2H), 2.47−2.58 (m, 8H), 7.27−7.29 (m, 6H), 7.78−7.82 (m, 2H), 8.03 (s, 2H), 13.57 (s, 2H). ^{19}F NMR (282 MHz, $CDCl_3$): δ −80.63. ^{13}C NMR (150 MHz, $CDCl_3$): δ 24.8, 24.9, 28.8, 29.5, 64.7, 65.4, 84.3 (q, J = 28.8 Hz), 117.7, 122.0, 123.4, 125.0, 125.7 (q, J = 283.5 Hz), 127.5, 127.6, 128.5, 129.4, 134.5, 152.8. HRMS Calcd for $C_{36}H_{37}N_4O_2F_6$ (MH^+): 671.2821. Found: 671.2831. Mp: 194 °C. $[\alpha]_D$ = −217.0 (c = 0.52, $CHCl_3$).

ASSOCIATED CONTENT

Supporting Information

NMR spectra of new compounds, additional optical spectra, and X-ray analysis data. This material is available free of charge via the Internet at http://pubs.acs.org.

AUTHOR INFORMATION

Corresponding Author

*E-mail: lp6n@virginia.edu.

Notes

The authors declare no competing financial interest.

■ ACKNOWLEDGMENTS

Partial support of this work from the U.S. National Science Foundation (CHE-0717995 and CHE-1047104) is gratefully acknowledged.

■ REFERENCES

(1) Herman, H. B.; Rechnitz, G. A. *Science* **1974**, *184*, 1074−1075.
(2) Meyerhoff, M. E.; Pretsch, E.; Welti, D. H.; Simon, W. *Anal. Chem.* **1987**, *59*, 144−150.
(3) (a) Wang, K.; Seiler, K.; Haug, J.-P.; Lehmann, B.; Hartman, S. W. K.; Simon, W. *Anal. Chem.* **1991**, *63*, 970−974. (b) Seiler, K.; Wang, K.; Kuratli, M.; Simon, W. *Anal. Chim. Acta* **1991**, *244*, 151−160.
(4) (a) Mohr, G. J.; Tirelli, N.; Lohse, C.; Spichiger-Keller, U. E. *Adv. Mater.* **1998**, *10*, 1353−1357. (b) Mertz, E.; Zimmerman, S. C. *J. Am. Chem. Soc.* **2003**, *125*, 3424−3425. (c) Sasaki, S.-i.; Kotegawa, Y.; Tamiaki, H. *Tetrahedron Lett.* **2006**, *47*, 4849−4852. (d) Ryu, D.; Park, E.; Kim, D.-S.; Yan, S.; Lee, J. Y.; Chang, B.-Y.; Ahn, K. H. *J. Am. Chem. Soc.* **2008**, *130*, 2394−2395.
(5) Sambasivan, S.; Kim, D.-S.; Ahn, K. H. *Chem. Commun.* **2010**, *46*, 541−543.
(6) Yu, S.; Plunkett, W.; Kim, M.; Pu, L. *J. Am. Chem. Soc.* **2012**, *134*, 20282−20285.
(7) For selected references on enantioselective fluorescent sensors, see: (a) James, T. D.; Sandanayake, K. R. A. S.; Shinkai, S. *Nature* **1995**, *374*, 345−347. (b) Pugh, V.; Hu, Q.-S.; Pu, L. *Angew. Chem., Int. Ed.* **2000**, *39*, 3638−3641. (c) Reetz, M. T.; Sostmann, S. *Tetrahedron* **2001**, *57*, 2515−2520. (d) Korbel, G. A.; Lalic, G.; Shair, M. D. *J. Am. Chem. Soc.* **2001**, *123*, 361−362. (e) Jarvo, E. R.; Evans, C. A.; Copeland, G. T.; Miller, S. J. *J. Org. Chem.* **2001**, *66*, 5522−5527. (f) Wong, W.-L.; Huang, K.-H.; Teng, P.-F.; Lee, C.-S.; Kwong, H.-L. *Chem. Commun.* **2004**, 384−385. (g) Zhao, J.-Z.; Fyles, T. M.; James, T. D. *Angew. Chem., Int. Ed.* **2004**, *43*, 3461−3464. (h) Pagliari, S.; Corradini, R.; Galaverna, G.; Sforza, S.; Dossena, A.; Montalti, M.; Prodi, L.; Zaccheroni, N.; Marchelli, R. *Chem.—Eur. J.* **2004**, *10*, 2749−2758. (i) Matsushita, H.; Yamamoto, N.; Meijler, M. M.; Wirsching, P.; Lerner, R. A.; Matsushita, M.; Janda, K. D. *Mol. BioSyst.* **2005**, *1*, 303−306. (j) Zhu, L.; Anslyn, E. V. *J. Am. Chem. Soc.* **2004**, *126*, 3676−3677. (k) Mei, X. F.; Wolf, C. *J. Am. Chem. Soc.* **2004**, *126*, 14736−14737.
(8) For reviews of enantioselective fluorescent recognition, see: (a) Pu, L. *Chem. Rev.* **2004**, *104*, 1687−1716. (b) Pu, L. *Acc. Chem. Res.* **2012**, *45*, 150−163. For a recent review of chiral optical sensors, see: (c) Leung, D.; Kang, S. O.; Anslyn, E. V. *Chem. Soc. Rev.* **2012**, *41*, 448−479.
(9) (a) Zhang, H.-C.; Huang, W.-S.; Pu, L. *J. Org. Chem.* **2001**, *66*, 481−487. (b) Cox, P.; Wang, W.; Snieckus, V. *Tetrahedron Lett.* **1992**, *33*, 2253−2256.
(10) Zhang, H.-C.; Pu, L. *Macromolecules* **2004**, *37*, 2695−2702.
(11) (a) Hou, S. Y.; Hetherington, W. M.; Korenowski, G. M.; Eisenthal, K. B. *Chem. Phys. Lett.* **1979**, *68*, 282−284. (b) Ford, D.; Thistlethwaite, P. J.; Woolfe, G. J. *Chem. Phys. Lett.* **1980**, *69*, 246−250.
(12) Forster, T. *Z. Electrochem.* **1950**, *54*, 531−534.
(13) Wan, P.; Shukla, D. *Chem. Rev.* **1993**, *93*, 571−584.
(14) Djoufac-Woumfo, E.; Arnaud, N.; Georges, J. *Analyst* **1988**, *113*, 447−450.
(15) Ofran, M.; Feitelson, J. *Chem. Phys. Lett.* **1973**, *19*, 427−431.
(16) Lee, J.; Griffin, R. D.; Robinson, G. W. *J. Chem. Phys.* **1985**, *82*, 4920−4925.
(17) Law, K.-Y.; Shoham, J. *J. Phys. Chem.* **1994**, *98*, 3114−3120.
(18) (a) Sasaki, S.-i.; Kotegawa, Y.; Tamiaki, H. *Tetrahedron Lett.* **2006**, *47*, 4849−4852. (b) Mertz, E.; Beil, J. B.; Zimmerman, S. C. *Org. Lett.* **2003**, *5*, 3127−3130.
(19) Tamborski, C.; Prabhu, U. D. G.; Eapen, K. C. *J. Fluorine Chem* **1985**, *28*, 139−150.
(20) Prakash, G. K. S.; Mathew, T.; Panja, C.; Vaghoo, H.; Venkataraman, K.; Olah, G. A. *Org. Lett.* **2007**, *9*, 179−182.